Charge-transfer salts with three different stoichiometries for the bimetallic molybdenum complex $CpMo(SMe)_4MoCp$ with TCNQ and $TCNQF_4$: structural and magnetic properties

Marc Fourmigué,*[a] Vincent Perrocheau,[a] Rodolphe Clérac[b] and Claude Coulon*[b]

[a]*Institut des Matériaux de Nantes (IMN), CNRS-Université de Nantes, 2, rue de la Houssinière, BP 32229, 44322 Nantes cedex 03, France*

[b]*Centre de Recherches Paul Pascal (CRPP), CNRS, Av. Dr. Schweitzer, 33600 Pessac, France*

The bimetallic complex $CpMo(SMe)_4MoCp$, **1**, oxidizes reversibly at 0.20 and 0.64 V *vs.* SCE. Reaction with TCNQ and $TCNQF_4$ leads to three crystalline phases of different stoichiometry, 1 : 2 in $\mathbf{1}\cdot(TCNQ)_2$, 2 : 1 in $\mathbf{1}_2\cdot TCNQ$ and 1 : 1 in $\mathbf{1}\cdot TCNQF_4$, whose crystal structures have been determined by single-crystal X-ray diffraction. Tetramerized TCNQ chains are present in $\mathbf{1}\cdot(TCNQ)_2$, separated from each other by $\mathbf{1}^{\bullet+}$ radical cations. This 2 : 1 salt exhibits semiconducting behavior ($\sigma_{RT} = 0.018$ S cm^{-1}). A transition is observed at 160 K in the spin susceptibility and in the EPR linewidth temperature dependence. Below this temperature only the Curie susceptibility of the non-interacting $\mathbf{1}^{\bullet+}$ cations remains. In the 2 : 1 $\mathbf{1}_2\cdot TCNQ$ salt, both neutral **1** and oxidized $\mathbf{1}^{\bullet+}$ coexist in the solid state, giving rise to alternating … $(\mathbf{1}^{\bullet+})(TCNQ^{\bullet-})(\mathbf{1}^{\bullet+})(TCNQ^{\bullet-})$ … chains while the empty spaces between the columns are filled with neutral donor molecules. Noticeable differences in the bond distances and angles between neutral **1** and oxidized $\mathbf{1}^{\bullet+}$ are identified and rationalized. No intermolecular interactions can be found in this compound, whose magnetism is best described by a Curie law for two independent $S = 1/2$ spins. In the 1 : 1 $TCNQF_4$ salt, uniform $TCNQF_4$ stacks are isolated from each other by a honeycomb net of $\mathbf{1}^{\bullet+}$ cations. Owing to the large interplanar $TCNQF_4$–$TCNQF_4$ distance [3.43(4) Å], the material behaves as a Mott insulator.

The observation of bulk ferromagnetism in a series of charge-transfer mixed-stack molecular crystals ($D^{\bullet+}$, $A^{\bullet-}$) based on metallocenium cations established a landmark in the development of molecular ferromagnets.[1] While the configuration interaction of degenerate orbitals with excited states was first considered to explain the ferromagnetic behavior of the alternated DADADA [Cp^*_2Fe][TCNE] salts,[2] the observation of ferromagnetism in the analogous chromocenium[3] and manganocenium salts[4,5] was also rationalized[6] using the concept of spin polarization, proposed by McConnell in 1963.[7] As a consequence, the presence of degenerate orbitals was no longer a prerequisite for possible ferromagnetic interactions. However, attempts to prepare other analogous ferromagnetic complexes have so far been restricted to the metal substitution in the metallocenium moiety and/or to the use of various acceptor moieties such as TCNQ, TCNE or metal dithiolene complexes.[8]

In our search for similar compounds, we have been interested in bimetallic complexes such as $CpMo(SMe)_4MoCp$, **1**,[9] and $CpMo(SCH_2CH_2S)_2MoCp$, **2**.[10] Those complexes have been reported to be easily oxidized to stable radical cation salts,[11] isolated with small closed-shell anions such as PF_6^- or BF_4^-. Furthermore their shape is reminiscent of that of metallocenes, with two parallel cyclopentadienyl planes available for π–π overlap. It was thus tempting to investigate the structural and magnetic properties of charge-transfer salts of **1** and **2** with electron-acceptor molecules such as TCNE, TCNQ and $TCNQF_4$. In the favorable case of mixed stack arrangement, Cp–TCNQ (or Cp–TCNE) p overlap may favor ferromagnetic interaction. Furthermore, these molecules can be easily modified by varying the nature of the substituents on the four sulfur atoms. In this paper, we describe the preparation, structural, magnetic and conductivity properties of a series of charge-transfer salts of **1** with TCNQ and $TCNQF_4$.

Results and Discussion

Synthesis and electrochemical behaviour

Compound **1** was prepared as previously described by King.[9] The isolation of the radical cation $\mathbf{1}^{\bullet+}$ has been reported by Connely and Dahl from chemical oxidation of **1** with $AgPF_6$, and structures of both **1** and $\mathbf{1}^{\bullet+}\cdot PF_6^-$ were described.[11]

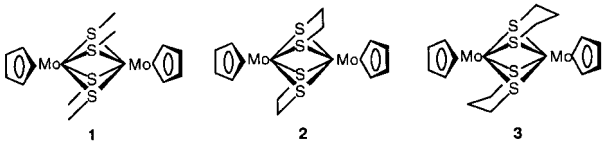

1 **2** **3**

This donor character was later substantiated by electrochemical studies on related compounds bearing two ethane-1,2-dithiolate (**2**) or propane-1,3-dithiolate groups (**3**) where reversible one-electron oxidations to the cation and dication were observed around 0.15 and 0.80 V *vs.* SCE.[10] However, the electrochemical characteristics of **1** were not reported in these studies and we thus undertook cyclic voltammetry measurements. Two reversible oxidation waves are indeed observed at 0.20 and 0.64 V *vs.* SCE, thus confirming the donor character of **1**. Note also that the reduction potentials of TCNQ ($E_{red} =$ 0.17 V *vs.* SCE) or TCNE ($E_{red} = 0.15$ V *vs.* SCE) are very close to, but smaller than this value. We can, however, expect that electron transfer will occur with the concomitant charge-transfer salt formation since, in the solid state, the Madelung energy in the ionic salt[12] can counteract this slightly unfavourable difference between the electron affinity (of TCNQ or TCNE) and the ionization potential of **1**, a difference roughly estimated by the difference between the redox potentials.[13] Lastly, $TCNQF_4$, which reduces at $E_{red} = 0.53$ V *vs.* SCE,[14] is expected to oxidize **1** without any doubt.

In fact, mixing equimolar solutions of **1** and one of those three acceptors led to an immediate color change from brown to green or blue, characteristic of the formation of the radical cation and anion. When equimolar quantities of **1** and TCNQ were used, a first crop of elongated needles was isolated, which proved to be a 1 : 2 phase, i. e. $\mathbf{1}\cdot(TCNQ)_2$. Further concentration and cooling of this TCNQ-deficient solution led to the crystallization of a 2 : 1 phase, *i.e.* $\mathbf{1}_2\cdot TCNQ$ as black parallelepipeds. These two phases were also obtained selectively by

using the required stoichiometry. With equimolar quantities of $TCNQF_4$, a 1:1 phase was isolated and characterized. However, no precipitation of crystalline material could be obtained from the reaction of **1** and TCNE. This may be because of either the unfavourable redox potential difference or high solubility of this salt, or both.

A variety of structural motifs

1·$(TCNQ)_2$ was found to crystallize in the triclinic system, space group $P\bar{1}$. One donor and two TCNQ molecules are located in general positions in the unit cell. Bond distances within the TCNQ moieties are in favor of a fractional charge transfer for both crystallographically independent molecules. From the correlations established by various authors between bond distances and charge transfer (ρ),[15] we found ρ values between -0.70 and -0.80 for TCNQ A and -0.40 and -0.60 for TCNQ B. Two IR stretching frequencies were found in the ν_{CN} region at 2197 and 2167 cm^{-1} together with a strong broad charge-transfer band centred around 3600 cm^{-1} and characteristic of partial charge transfer.[16] In the cationic $\mathbf{1}^{\bullet+}$ moiety, the sulfur atoms were found to be disordered, giving rise to two sets of four sulfur atoms with a 50:50 population (see Experimental). However each methyl group was found to be non-disordered in that the positions of the two methyl carbon atoms of each disordered pair of sulfur atoms were assumed to be coincident (Fig. 1). This particular disorder model was already mentioned in the structures of **1** and **1**·PF_6 and appears to be a permanent feature of this molecule (see below). In the crystal, the $TCNQ^{\bullet-}$ radical anions stack on top of each other, giving rise to tetramerized chains along the *b* direction (Fig. 2). Indeed, three interplanar TCNQ–TCNQ distances can be identified, with three different overlap patterns (Fig. 3). Within the tetramer they exhibit the characteristic bond-over-ring pattern observed in most mixed-valence TCNQ dimers while, between tetramers, the overlap pattern shows a much larger longitudinal displacement. The calculated LUMO–LUMO intermolecular interaction energies, which are a measure of the strength of the interaction between two TCNQ LUMOs in adjacent positions,[17] are given in Fig. 3 and confirm the electronically tetramerized character of the chains. Indeed, within a tetrameric unit the β_{ij} values are nearly identical while they are only half as large between the tetramers. Note that despite an apparently small AA overlap [Fig. 3(c)], the shorter plane-to-plane distance (Fig. 2) together with the presence of a large coefficient in the TCNQ LUMO [Fig. 3(d)] at the overlapping carbon atom induces a comparatively non-negligable interaction between tetramers.

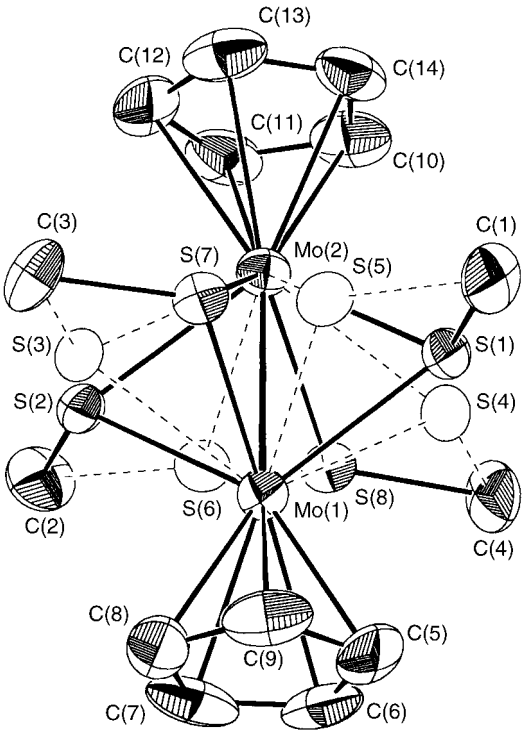

Fig. 1 ORTEP view of $\mathbf{1}^{\bullet+}$ in **1**·$(TCNQ)_2$

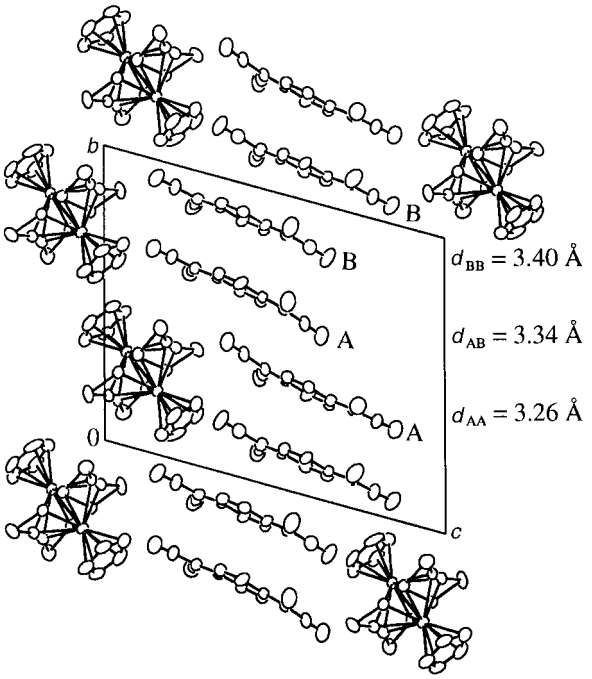

Fig. 2 Projection of the structure of **1**·$(TCNQ)_2$ on the *bc* plane, showing the tetramerized TCNQ stack. The three independent interplanar TCNQ–TCNQ distances are given.

A second TCNQ phase was obtained by concentration of the mother liquors from the former reaction to give black parallelepipedic crystals. The same phase was also obtained directly from the reaction of two equivalents of **1** with one equivalent of TCNQ. It crystallizes in the monoclinic system, space group $P2_1/c$ with an unusual[18] 2:1 stoichiometry, *i.e.*, two donor molecules for one TCNQ molecule. One TCNQ and two independent donor molecules (D1 and D2) are located on inversion centers, molecule D1 [built on Mo(1)] at (1/2,0,0) and molecule D2 [built on Mo(2)] at (0,0,0) (Fig. 4). Bond distances within the TCNQ moiety are indicative of complete charge transfer, as also confirmed by the IR ν_{CN} at 2177 and 2151 cm^{-1}. The lack of a broad charge-transfer band confirms the absence of any π–π $TCNQ^{\bullet-}$–$TCNQ^{\bullet-}$ interaction. The sulfur atoms of **1** in molecules D1 and D2 exhibit positional disorder analogous to that already mentioned. Refinement of the population parameters of the two sets of sulfur atoms converges here to a 60:40 and 70:30 distribution for molecules D1 and D2 respectively.

The problem we are now faced with concerns the oxidation state of molecules D1 and D2 in this salt, a mixed-valence $D1^{1/2+}$ $D2^{1/2+}$ state or a coexistence of both **1** and $\mathbf{1}^{\bullet+}$ in the solid state? And in the latter case, of the two structurally independent molecules D1 and D2, which is the oxidized one? Relevant bond distances and angles for this bimetallic complex in different compounds are collected in Table 1. It appears that: (i) oxidation of **1** to the radical cation does indeed modify its geometry, with a small increase of both the Mo—Mo distance and the Mo—S—Mo angles, (ii) both **1** and $\mathbf{1}^{\bullet+}$ coexist in the 2:1 $\mathbf{1}_2$·TCNQ salt, with molecule D1 to be

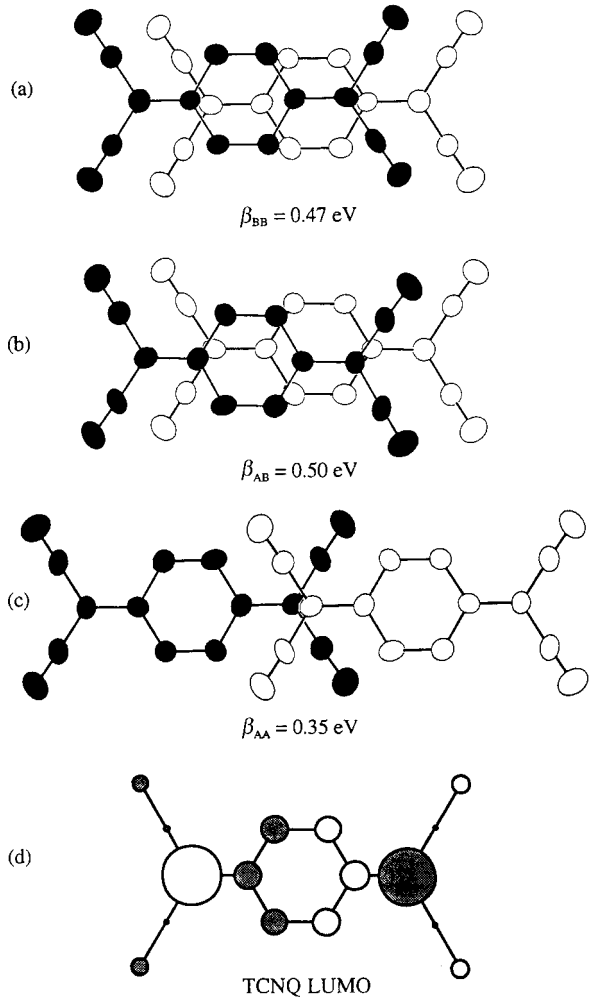

Fig. 3 (*a*)–(*c*) Molecular overlaps in the columnar stacking of TCNQ anions. The view direction is normal to the least-squares molecular planes. The calculated overlap interaction energies β_{ij} are also given. (*d*) The LUMO of TCNQ as seen from above. Only the upper lobe of each p AO is shown.

considered as neutral **1** and molecule D2 to be considered as oxidized $\mathbf{1}^{\bullet+}$. These geometrical changes upon electron counting are the subject of several recent studies[19] and can be rationalized with help of extended Hückel calculations. Indeed, in these systems it has been shown[20] that the six available electrons (two Mo^{III}) occupy one bonding σ and both the bonding δ and antibonding δ^* metal orbitals, with the δ orbital above the δ^*. Thus, removal of one electron from the weakly bonding δ orbital is expected to give rise to a small Mo—Mo bond weakening and lengthening, accompanied by a Mo—S—Mo angle increase, as observed here (Table 1).

With these results in hand, we are now able to identify in the structure of $\mathbf{1}_2$·TCNQ, chains of alternating $\mathbf{1}^{\bullet+}$ and

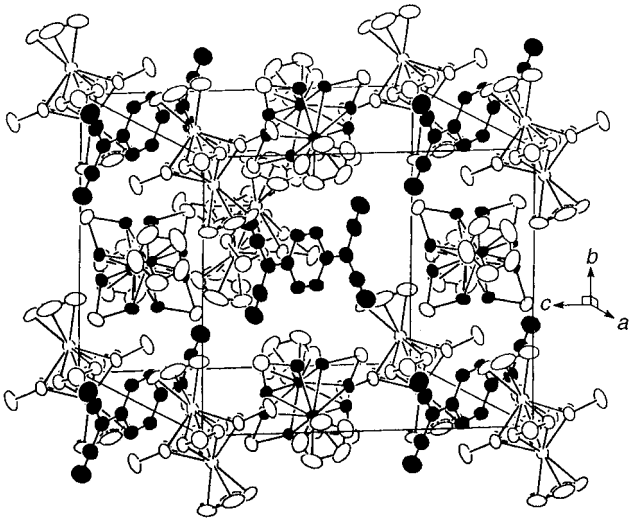

Fig. 4 A view of the unit cell of $\mathbf{1}_2$·TCNQ. The TCNQ molecules and molybdenum and sulfur atoms of the neutral donor molecules (D1 in text) are shown in black. The oxidized D2 molecule lying at the center of the foremost *bc* face has been omitted for clarity.

$TCNQ^{\bullet-}$ running along [100] at the edges and the center of the unit cell (Fig. 4). Those columns are narrowed at the positions of the smaller $TCNQ^{\bullet-}$ anions, leaving empty spaces between them, occupied by the neutral donor molecules. Note that the planar $TCNQ^{\bullet-}$ and cyclopentadienyl moieties of $\mathbf{1}^{\bullet+}$ are not parallel. Thus, very limited overlap between radical anions and cation radicals can be expected here.

1·$TCNQF_4$ crystallizes in the orthorhombic system, space group *Pbcn*. $TCNQF_4^{\bullet-}$ radical anions are located on inversion centers while $\mathbf{1}^{\bullet+}$ cations are located on the twofold axis along [010] (Fig. 5). From this site symmetry, the population parameter of the two sets of disordered sulfur atoms is imposed here at 50:50. Bond distances within the $TCNQF_4^{\bullet-}$ anion confirm complete charge transfer while bond distances and angles in $\mathbf{1}^{\bullet+}$ are in accord with those found above for the $\mathbf{1}^{\bullet+}$ radical cation (Table 1). In the structure, $TCNQF_4^{\bullet-}$ anions are organized in uniform chains running along [001] with a rare crosswise mode of overlap and a large plane-to-plane distance of 3.43(4) Å. Thus the strong tendency of $TCNQF_4^{\bullet-}$ radical anions to dimerize into diamagnetic $(TCNQF_4)_2^{2-}$ systems, in isolated dimers[21] as well as in dimerized chains,[22] is not observed here. Furthermore, the plane-to-plane distance is intermediate between intra- (*ca.* 3.2 Å) and inter-dimer (3.55–3.7 Å) distances usually found in dimerized $TCNQF_4^{\bullet-}$ chains. These chains are completely isolated from each other by $\mathbf{1}^{\bullet+}$ cations who form an hexagonal honeycomb network (Fig. 6) and it is thus possible that this compact hexagonal array of $\mathbf{1}^{\bullet+}$ cations forces the regular chain arrangement observed here for the $TCNQF_4^{\bullet-}$ anions.

Table 1 Relevant bond distances (Å) and angles (°) for **1** in different compounds

	neutral **1**	$\mathbf{1}^{\bullet+}$ in **1**·PF_6	$\mathbf{1}^{\bullet+}$ in **1**·$(TCNQ)_2$	$\mathbf{1}^{\bullet+}$ in **1**·$TCNQF_4$	D1 in $\mathbf{1}_2$·TCNQ	D2 in $\mathbf{1}_2$·TCNQ
distances						
Mo—Mo	2.603(2)	2.617(4)	2.629(1)	2.6305(7)	2.6098(7)	2.6343(8)
Mo—S	2.46	2.44	2.44(1)	2.44(1)	2.462(6)	2.444(9)
S···S	2.96	2.90	2.912(8)	2.917(9)	2.95(2)	2.91(1)
S—CH_3	1.84	1.82	1.81(2)	1.784(9)	1.85(1)	1.80(2)
Mo—Cp	1.97	1.97	1.982(2)	1.977(1)	1.981(1)	1.980(2)
angles						
Mo—S—Mo	64	65	65.1(3)	65.1(1)	65.2(1)	65.1(3)
S—Mo—S	116	115	114.9(5)	114.9(5)	116.0(1)	114.8(1)

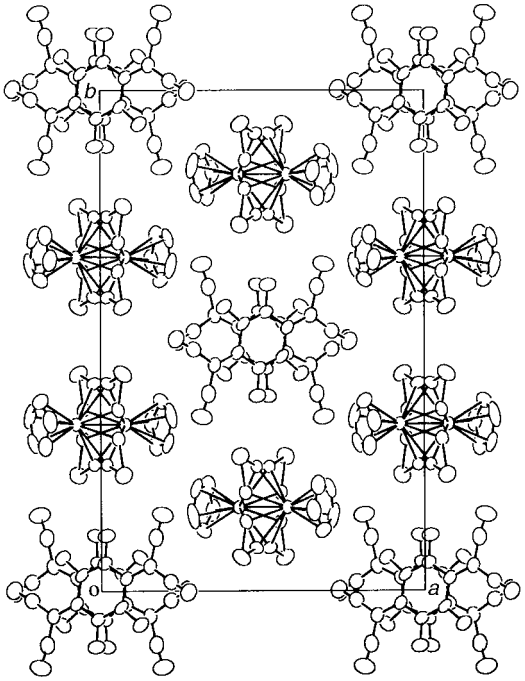

Fig. 5 A projection along the *c* axis of **1**·$TCNQF_4$. Note the hexagonal array of $\mathbf{1}^{\bullet+}$ cations around the $TCNQF_4$ stacks.

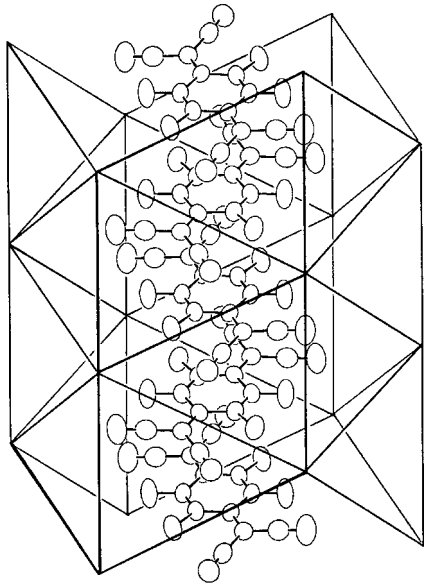

Fig. 6 A view of a $TCNQF_4$ stack surrounded by the hexagonal network of donor molecules. Each point of the net is located at the barycentre of $\mathbf{1}^{\bullet+}$ cations.

Electronic properties: combined EPR, susceptibility and conductivity studies.

In the 1:2 TCNQ salt, **1**·$(TCNQ)_2$, one single EPR resonance line is observed, with extrema of the g tensor values at $g_{max}=2.0125$, $g_{int}=2.0111$ and $g_{min}=1.9990$. The anisotropy of the $\boldsymbol{g}$ tensor demonstrates the participation of the radical cation $\mathbf{1}^{\bullet+}$ in the EPR signal since the $\boldsymbol{g}$ tensor of $TCNQ^{\bullet-}$ is well known to be quasi-isotropic around $g=2.0033$. A sharp transition is observed at 160 K, in both the linewidth and *g*-value temperature dependence with a small hysteresis (Fig. 7). Similarly, (Fig. 8), two regimes are identified in the SQUID susceptibility data (obtained from a polycrystalline sample of 21.4 mg at 1 T). In the low temperature regime, χT is nearly constant and the susceptibility can be represented by a Curie law with

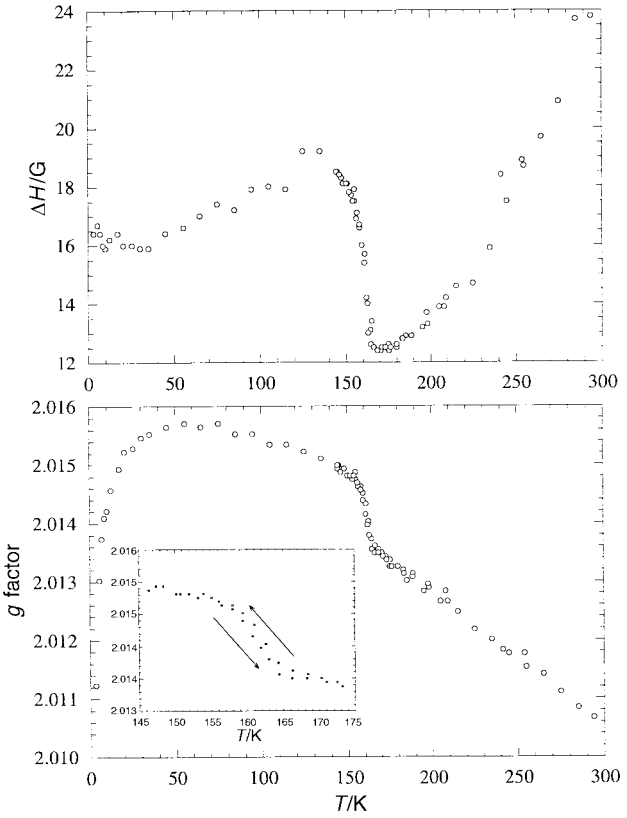

Fig. 7 Temperature dependence of the EPR linewidth and *g* values in **1**·$(TCNQ)_2$

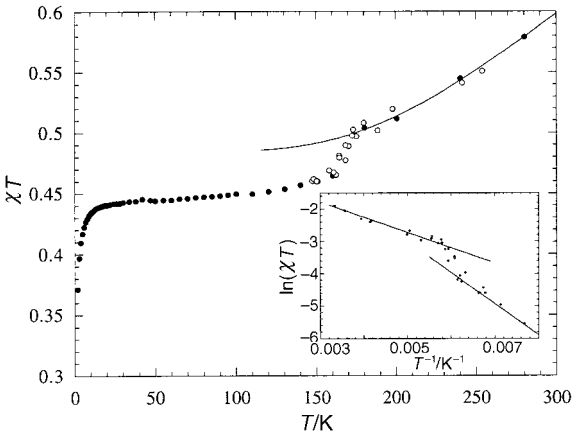

Fig. 8 Temperature dependence of χT [emu(CGS) K mol^{-1}] in **1**·$(TCNQ)_2$. The solid line is a fit of the data to the high-temperature singlet–triplet contribution to the susceptibility. Black dots are SQUID measurements and white dots come from the EPR susceptibility (through integration and normalization of the EPR signal). Insert: $\ln(\chi T)$ *vs.* T^{-1} between 130 K and room temperature.

one spin $S=1/2$ per **1**·$(TCNQ)_2$ moiety, attributable to the $\mathbf{1}^{\bullet+}$ cations. The extra susceptibility observed in the high temperature regime is thermally activated and a plot of $\ln(\chi T)$ *vs.* $1/T$ (Fig. 8, insert) shows a linear dependence with two different activation energies, $J_1/k=470$ K above 160 K, $J_2/k=965$ K below 160 K. Single crystal conductivity measurements performed on two different crystals show that **1**·$(TCNQ)_2$ is a semiconductor, with $\sigma_{RT}=0.018\ S\ cm^{-1}$ and an activation energy at room temperature of 0.07 eV. The crystals become very insulating at lower temperatures and their resistivity could not be measured below 180 K. These results show that the high temperature contribution to the susceptibility arises from two antiferromagnetically coupled spins within each $(TCNQ)_4^{2-}$ tetramer. The singlet–triplet behavior observed at

room temperature with $J_1/k = 470$ K is modified upon cooling by a structural transition around 160 K which changes (i) the molecular geometry and orientation of the $TCNQ^{\bullet -}$ radical anions (the g value changes abruptly), and (ii) the TCNQ–TCNQ overlaps (the energy gap is modified). This behavior is reminiscent of the thoroughly investigated $TEA(TCNQ)_2$ (TEA = triethylammonium), where tetramerized chains exhibit a similar semiconductor–semiconductor transition.[23]

One single EPR resonance line is observed on a single crystal of the 2:1 TCNQ salt, $\mathbf{1}_2 \cdot TCNQ$. From six independent g values, we deduce extrema of the $\boldsymbol{g}$ tensor as $g_{max} = 2.0076$, $g_{int} = 2.0059$ and $g_{min} = 2.0006$. The g_{max} and ΔH values vary slightly with temperature down to 25 K while an increase of both parameters can be observed below 25 K (Fig. 9). This may be attributable to antiferromagnetic fluctuations but the nearly perfect Curie law behavior (see below) would rule out this hypothesis. Indeed, from the SQUID data (obtained at 1 T on a polycrystalline sample weighing 21.5 mg), Curie law behavior is deduced, with a Curie constant of 0.8 emu (CGS) K mol^{-1} (Fig. 10) compatible with the presence of two independent $S = 1/2$ spins. Thus, as already suspected from the structural arrangement in $\mathbf{1}_2 \cdot TCNQ$ and the absence of any sizeable overlap between donor and acceptor moieties, there is no noticeable interaction between $\mathbf{1}^{\bullet +}$ radical cations and $TCNQ^{\bullet -}$ radical anions along those DADADA chains.

Finally, in $\mathbf{1} \cdot TCNQF_4$, one single EPR line is also observed with extrema of the g values along the needle-like crystal [001] axis ($g_{int} = 2.0096$) and in the plane perpendicular to [001] with $g_{max} = 2.0114$ and $g_{min} = 1.999$. The linewidth (ΔH) is slightly anisotropic with ΔH values of 34.5, 36 and 47 G in the g_{max}, g_{int} and g_{min} orientations, respectively, and its variation with temperature shows a minimum around 150 K (Fig. 11 insert). The SQUID susceptibility data (at 1 T on a polycrystalline sample weighing 25.4 mg) can be fitted with a Curie law in the low temperature regime (below 150 K) with a Curie

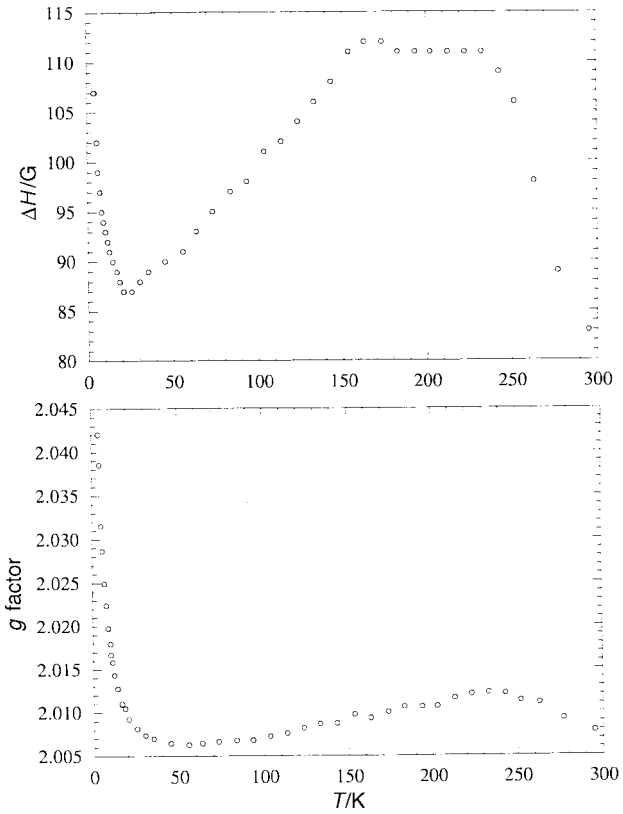

Fig. 9 Temperature dependence of the EPR linewidth and the g_{max} value in $\mathbf{1}_2 \cdot TCNQ$

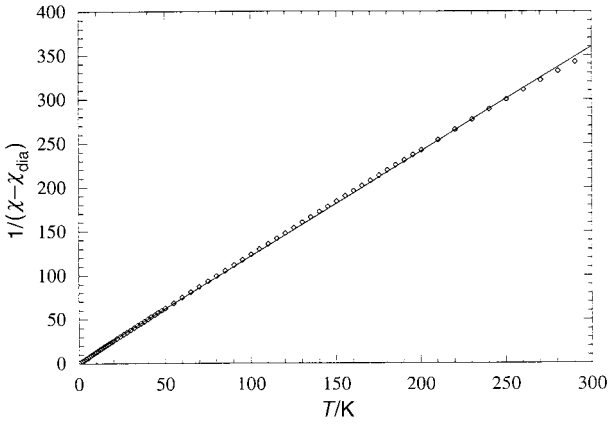

Fig. 10 $1/\chi$ [emu(CGS)$^{-1}$ mol] *vs.* T in $\mathbf{1}_2 \cdot TCNQ$. The solid line is a linear fit to the data giving a Curie constant of 0.8 emu(CGS) K mol^{-1}.

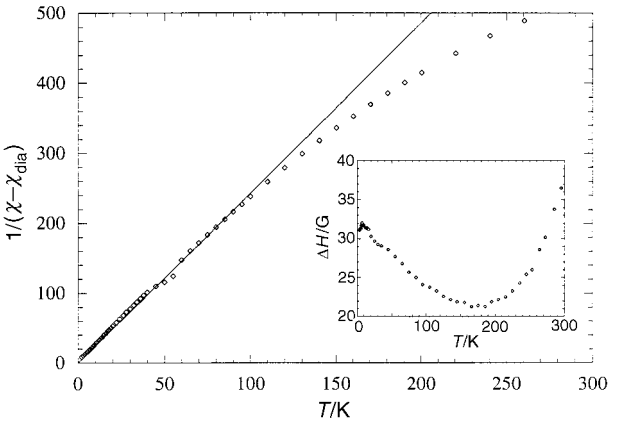

Fig. 11 $1/\chi$ [emu(CGS)$^{-1}$ mol] *vs.* T in $\mathbf{1} \cdot TCNQF_4$. The solid line is a linear fit in the low temperature regime giving a Curie constant of 0.4 emu(CGS) K mol^{-1}. Insert: temperature dependence of the single crystal EPR linewidth.

constant of 0.4, compatible with the presence of one $S = 1/2$ spin, very probably originating from the $\mathbf{1}^{\bullet +}$ radical cations (Fig. 11). The small extra susceptibility observed above 150 K is therefore attributable to the $TCNQF_4^{\bullet -}$ anions contribution to the susceptibility. The temperature dependence of the EPR linewidth (Fig. 11 insert) can thus be described as the sum of two terms whose temperature dependences are opposite. The high temperature ΔH increase would be related to interacting electrons of the $TCNQF_4^{\bullet -}$ chains, while in the low temperature regime ΔH increases with decreasing T as often observed for non-interacting Curie-type spins.

As described above, a uniform chain $(TCNQF_4^{\bullet -})_n$ was observed in the room-temperature X-ray crystal structure with a plane-to-plane distance of 3.43(1) Å. This distance, close to the van der Waals radius for an aromatic ring, can be considered as large for TCNQ (and $TCNQF_4$)[24] salts and is indeed comparable to distances observed in the high temperature phases of insulating 1:1 TCNQ salts such as K·TCNQ[25] or Rb·TCNQ.[26] These compounds, described as Mott insulators, are associated with large U coulombic interactions.[27] Actually, single crystal conductivity measurements indicate that $\mathbf{1} \cdot TCNQF_4$ is an insulator, and neither a Bonner–Fischer uniform chain susceptibility model nor a singlet–triplet model reproduce satisfactorily the excess susceptibility observed above 150 K. Thus, we might consider the $TCNQF_4$ subsystem of $\mathbf{1} \cdot TCNQF_4$ as a Mott insulator at room temperature, which undergoes a structural transition upon cooling.

Table 2 Crystallographic data

	1·$(TCNQ)_2$	$\mathbf{1}_2$·TCNQ	**1**·$TCNQF_4$
formula	$C_{38}H_{30}Mo_2N_8S_4$	$C_{40}H_{48}Mo_4N_4S_8$	$C_{26}H_{22}F_4Mo_2N_4S_4$
M_r	918.854	1225.136	786.625
crystal dimensions/mm	$0.36\times0.18\times0.02$	$0.27\times0.18\times0.12$	$0.42\times0.15\times0.10$
crystal shape	platelet	parallelepiped	needle
T/K	293	293	293
cystal system	triclinic	monoclinic	orthorhombic
space group	$P\bar{1}$	$P2_1/c$	$Pbcn$
a/Å	7.814(3)	12.0575(8)	15.793(2)
b/Å	14.373(1)	13.374(2)	24.033(2)
c/Å	17.497(2)	15.618(1)	7.7240(8)
α/degrees	104.967(7)	90	90
β/degrees	93.58(1)	111.151(7)	90
γ/degrees	95.38(1)	90	90
V/Å^3	1882.3(7)	2348.9(4)	2931.7(5)
Z	2	2	4
d_{calc}/g cm^{-3}	1.60	1.73	1.78
μ/mm^{-1}	0.93	1.43	1.19
scan width/degrees	$1+0.35\tan\theta$	$1+0.35\tan\theta$	$1+0.35\tan\theta$
$2\theta_{max}$/degrees	52	60	56
h,k,l limits	$+9, \pm17, \pm21$	$+16, +18, \pm21$	$+20, +30, +10$
data collected	7966	7317	4894
independent data	7392	6826	3524
R_{int}	0.020	0.012	0.027
observed data $[I_{obs}>3\sigma(I)]$	3558	3910	1755
data used	3731	4055	1823
param. refined	459	291	199
R^a, $R_w{}^b$	0.042, 0.055	0.039, 0.057	0.041, 0.056
GOF, S^c	1.04	1.10	1.08
final shift/error	0.04	0	0.09
residual density/e Å^{-3}	1.2, −2.7	1.4, −2.1	1.35, −1.75

$^aR=\Sigma||F_o|-|F_c||/\Sigma|F_o|$. $^bR_w=[\Sigma w(|F_o|-|F_c|)^2/\Sigma w|F_o|^2]^{1/2}$. $^cS=[\Sigma w(F_o{}^2-F_c{}^2)^2/(N_{obs}-N_{var})]^{1/2}$.

Conclusion

In each of the three systems described here, the absence of any π–π interaction between donor and acceptor moieties leads to a simple addition of the magnetic contributions of both cationic and anionic sub-systems. The partial ($\rho=0.5$) charge transfer in **1**·$(TCNQ)_2$ leads to semiconducting tetramerized TCNQ chains; the total ($\rho=1$) charge transfer in **1**·$TCNQF_4$, together with large coulombic interactions, gives rise to a Mott insulator. Both anionic sub-systems undergo a transition to a non-magnetic ground state while the non-interacting $\mathbf{1}^{\bullet+}$ cations exhibit Curie law behavior in the whole temperature range. Finally, in $\mathbf{1}_2$·TCNQ, non-interacting $\mathbf{1}^{\bullet+}$ and $TCNQ^{\bullet-}$ lead to a Curie law with two spins per $\mathbf{1}_2$·TCNQ moiety. These electronic properties are the direct consequence of the structural characteristics of those salts and we suspect that the small size of the Cp rings probably does not favor the parallel arrangement of the cyclopentadienyl and acceptor moieties which would eventually give rise to sizeable intermolecular interactions. Work is currently in progress to prepare for example the analogous complexes with larger Cp* substituents.

This work was supported by the CNRS and the Région Pays de Loire. V. P. is a student from the Insitut Universitaire de Technologie (IUT) in Le Mans, France. We thank P. Auban-Senzier, at the Laboratoire de Physique des Solides, Université Paris-Sud, Orsay, France, for the conductivity measurements.

Experimental

Synthesis

Compound **1** was prepared as previously described from $[CpMo(CO)_3]_2$ and MeSSMe in refluxing heptane.[9] Commercially available TCNQ was sublimed before use and $TCNQF_4$ was prepared according to published procedures.[28]

1·$(TCNQ)_2$ was prepared as follows. Hot solutions of TCNQ (10 mg, 0.049 mmol) in dry CH_3CN and **1** (25 mg, 0.049 mmol) in toluene–CH_3CN were combined and the resulting green solution cooled to room temperature and then at −18 °C for 3 days. Deposited black platelets were filtered and washed with a small amount of CH_3CN. [Found: C, 49.23; H, 3.06; N, 12.05. $C_{38}H_{30}Mo_2N_8S_4$ requires C, 49.67; H, 3.29; N, 12.19%]. The concentrated solution, left again overnight at −18 °C, afforded a second crop of parallelepipedic crystals which proved to be the 2:1 salt (see below).

$\mathbf{1}_2$·TCNQ was obtained quantitatively in the same conditions as above using only 0.5 equivalents of TCNQ. [Found: C, 38.96; H, 3.94; N, 4.67. $C_{40}H_{40}Mo_4N_4S_8$ requires C, 39.22; H, 3.95; N, 4.57%].

1·$TCNQF_4$ was obtained analogously from $TCNQF_4$ (13.5 mg, 0.049 mmol) dissolved in CH_3CN and **1** (25 mg, 0.049 mmol) dissolved in toluene–CH_3CN. After cooling at −18 °C, a first crop of large needles was isolated. The concentrated solution, left at −18 °C overnight afforded a second crop of the same compound. [Found: C, 39.68; H, 2.91; N, 7.34. $C_{26}H_{22}F_4Mo_2N_4S_4$ requires C, 39.70; H, 2.82; N, 7.12%].

Electrochemical measurements

Cyclic voltammograms were recorded on a PAR 273 potentiostat with Pt working (1 mm^2) and auxiliary (1 cm^2) electrodes, a SCE reference electrode and $Bu^n{}_4N^+PF_6{}^-$ as supporting electrolyte at a scan rate of 100 mV s^{-1}. Solvents were dried over basic aluminium oxide before use.

X-Ray crystallography

Experimental details for **1**·$(TCNQ)_2$, $\mathbf{1}_2$·TCNQ and **1**·$TCNQF_4$ are given in Table 2.† Precise unit-cell dimensions and intensity

† Atomic coordinates, thermal parameters, and bond lengths and angles have been deposited at the Cambridge Crystallographic Data Centre (CCDC). See Information for Authors, *J. Mater. Chem.*, 1997, Issue 1. Any request to the CCDC for this material should quote the full literature citation and the reference number 1145/48.

data were collected on an Enraf-Nonius Mach3 diffractometer, using Mo-Kα radiation ($\lambda = 0.710\,73$ Å). The unit-cell dimensions and crystal orientation matrix were derived from least-squares refinement of setting angles of 25 reflections. Intensity data were collected in the ω–2θ mode.

Absorption corrections were applied using empirical procedures based on azimuthal ψ-scans (ABSCAL, Xtal3.2). The structures were solved by direct methods and successive Fourier differences, using the Xtal3.2 system of programs.[29]

Structure solutions

In the three structures, the four bridging sulfur atoms of **1** were found to be disordered such that there are two sets of four sulfur atoms (see Fig. 1). However, each methyl group was found to be non-disordered in that the positions of the two methyl carbon atoms of each disordered pair of sulfur atoms were assumed to be coincident. The presumably disordered hydrogen atoms were neither located nor introduced at calculated positions.

In **1**·$TCNQ_2$, $\mathbf{1}^{\bullet+}$ is located in a general position in the unit cell. The population of the two sulfur sets was refined while the U_{iso} of the sulfur atoms was constrained to a unique value. The population parameters converged toward 0.49 and 0.51. These population parameters were thus both fixed at 0.50 and all atoms including sulfur atoms were then refined anisotropically.

In $\mathbf{1}_2$·TCNQ, two independent donor molecules, identified (see text) as neutral **1** and oxidized $\mathbf{1}^{\bullet+}$, are located on inversion centers. Thus the populations of the two independent sulfur sets were refined for **1** and $\mathbf{1}^{\bullet+}$ while the U_{iso} of the sulfur atoms was constrained to a unique value. The population parameters converged toward 0.60 and 0.40 in neutral **1** and 0.70 and 0.30 in oxidized $\mathbf{1}^{\bullet+}$. These population parameters were thus fixed and all atoms including sulfur atoms were then refined anisotropically.

In **1**·$TCNQF_4$, $\mathbf{1}^{\bullet+}$ is located on a twofold axis, the population parameters of the two sulfur sets were therefore then fixed by symmetry at 0.50 each.

Magnetic measurements

Single-crystal EPR measurements were performed on a Bruker ESP300E spectrometer equipped with an ESR900 cryostat (4.2–300 K) from Oxford Instruments. Magnetic susceptibility measurements on polycrystalline samples were made with a Quantum Design MPMS-5 SQUID magnetometer in the range 1.7–300 K.

Conductivity measurements

The temperature dependence of the conductivity of **1**·$TCNQ_2$ and **1**·$TCNQF_4$ was measured on single crystals at ambient pressure using a four-probe technique with evaporated gold contacts.

Interaction energy calculations

Extended Hückel type calculations[30] were performed with double-ζ orbitals for C, N and F.[31] The β_{ij} interaction energy between two orbitals i and j is defined as

$$\beta_{ij} = \sum_{\mu}\sum_{\nu} c_{\mu i}c_{\nu j}\langle\chi_{\mu}|H^{\text{eff}}|\chi_{\nu}\rangle$$

where $c_{\mu i}$ is the coefficient of atomic orbital χ_{μ} in the molecular orbital Ψ_i with $\Psi_i = \sum_{\mu} c_{\mu i}\chi_{\mu}$.

References

1 J. S. Miller and A. J. Epstein, *Angew. Chem., Int. Ed. Engl.*, 1994, **33**, 385.
2 (*a*) H. M. McConnell, *Proc. R. A. Welch Found. Conf.*, 1967, **11**, 144; (*b*) J. S. Miller, A. J. Epstein and W. M. Reiff, *Chem. Rev.*, 1988, **88**, 201; (*c*) J. S. Miller and A. J. Epstein, *J. Am. Chem. Soc.*, 1987, **109**, 3850; (*d*) J. S. Miller, A. J. Epstein and W. M. Reiff, *Science*, 1988, **240**, 40.
3 (*a*) W. E. Broderick and B. M. Hoffman, *J. Am. Chem. Soc.*, 1991, **113**, 6334; (*b*) D. M. Heichhorn, D. C. Skee, W. E. Broderick and B. M. Hoffman, *Inorg. Chem.*, 1993, **32**, 491.
4 W. E. Broderick, J. A. Thompson, E. P. Day and B. M. Hoffman, *Science*, 1990, **249**, 401.
5 G. T. Yee, J. M. Manriquez, D. A. Dixon, R. S. McLean, D. M. Groski, R. B. Flippen, K. R. Narayan, A. J. Epstein and J. S. Miller, *Adv. Mater.*, 1991, **3**, 309.
6 (*a*) A. L. Buchachenko, *Mol. Cryst. Liq. Cryst.*, 1989, **176**, 369; (*b*) C. Kollmar, M. Couty and O. Kahn, *J. Am. Chem. Soc.*, 1991, **111**, 7994; (*c*) C. Kollmar and O. Kahn, *J. Chem. Phys.*, 1992, **96**, 2988.
7 H. M. McConnell, *J. Chem. Phys.*, 1963, **39**, 1910.
8 W. E. Broderick, J. A. Thompson and B. M. Hoffman, *Inorg. Chem.*, 1991, **30**, 2958.
9 R. B. King, *J. Chem. Soc.*, 1963, 1587.
10 M. Rakowski-Dubois, R. C. Haltiwanger, D. J. Miller and G. Glatzmaier, *J. Am. Chem. Soc.*, 1979, **101**, 5245.
11 N. G. Connely and L. F. Dahl, *J. Am. Chem. Soc.*, 1970, **92**, 7470.
12 J. B. Torrance, *Acc. Chem. Res.*, 1979, **12**, 79.
13 R. O. Loufty and Y. C. Cheng, *J. Chem. Phys.*, 1980, **73**, 2902.
14 R. C. Wheland and J. L. Gillson, *J. Am. Chem. Soc.*, 1976, **98**, 3916.
15 (*a*) S. Flandrois and D. Chasseau, *Acta Crystallogr., Sect. B*, 1977, **33**, 2744; (*b*) T. J. Kistenmacher, T. J. Emge, A. N. Bloch and D. O. Cowan, *Acta Crystallogr., Sect. B*, 1982, **38**, 1193; (*c*) T. C. Umland, S. Allie, T. Kuhlman and P. Coppens, *J. Phys. Chem.*, 1988, **92**, 6456.
16 J. B. Torrance, B. A. Scott, B. Welber, F. B. Kaufman and P. E. Seiden, *Phys. Rev. B*, 1979, **19**, 730.
17 See for example: J. M. Williams, H. H. Wang, T. Emge, U. Geiser, M. A. Beno, P. C. W. Leung, K. D. Carlson, A. J. Schultz and M.-H. Whangbo, *Prog. Inorg. Chem.*, 1987, **35**, 51.
18 A Cambridge Structutal Database search on TCNQ salts afforded 442 structures of which only 10 exhibited this peculiar 2 : 1 stoichiometry, *i.e.* two donor molecules per TCNQ molecules. Furthermore, most of those complexes are not ionic salts but neutral charge transfer complexes, with weak donor molecules such as perylene with DDADDADDA arrangements.
19 See for example: (*a*) M. Fourmigué and C. Coulon, *Adv. Mater.*, 1994, **6**, 948; (*b*) M. Fourmigué, C. Lenoir, C. Coulon, F. Guyon and J. Amaudrut, *Inorg. Chem.*, 1995, **34**, 4979 and references therein.
20 W. Tremel, R. Hoffmann and E. D. Jemmis, *Inorg. Chem.*, 1989, **28**, 1213.
21 (*a*) M. D. Ward and D. C. Jonhson, *Inorg. Chem.*, 1987, **26**, 4213; (*b*) R. M. Metzger, N. E. Heimer, D. Gundel, H. Sixl, R.H. Harms, H. J. Keller, D. Nöthe and D. Wehe, *J. Chem. Phys.*, 1982, **77**, 6203.
22 (*a*) F. M. Wiygul, T. J. Emge and T. J. Kistenmacher, *Mol. Cryst. Liq. Cryst.*, 1982, **90**, 163; (*b*) T. J. Emge, W. A. Bryden, F. M. Wuygul, D. O. Cowan, T. J. Kistenmacher and A. N. Bloch, *J. Chem. Phys.*, 1982, **77**, 3188. (*c*) J. S. Miller, J. H. Zhang and W. M. Reiff, *Inorg. Chem.*, 1987, **26**, 600.
23 (*a*) A. Filhol and M. Thomas, *Acta Crystallogr., Sect. B*, 1984, **40**, 44; (*b*) A Brau and J.-P. Farges, *Phys. Status Solidi B*, 1974, **61**, 257.
24 The van der Waals radius of fluorine (1.35 Å) is much smaller than that of the aromatic moiety. Thus the fluorine substitution is not expected to interfere in the π–π stacking.
25 M. Konno, T. Ishii and Y. Saito, *Acta Crystallogr., Sect. B*, 1977, **33**, 763.
26 A. Hoekstra, T. Spoelder and A. Vos, *Acta Crystallogr., Sect. B*, 1972, **28**, 14.
27 J. B. Torrance, *Ann. N. Y. Acad. Sci.*, 1978, **313**, 210.
28 R. C. Wheland and E. L. Martin, *J. Org. Chem.*, 1975, **40**, 3101.
29 Xtal3.2, S. R. Hall, H. D. Flack and J. M. Stewart, Universities of Western Australia, Geneva and Maryland, 1992.
30 R. Hoffmann, *J. Chem. Phys.*, 1963, **39**, 1397.
31 (*a*) M.-H. Whangbo, J. M. Williams, P. C. W. Leung, M. A. Beno, T. J. Emge, H. H. Wang, K. D. Carlson and G. W. Crabtree, *J. Am. Chem. Soc.*,1985, **105**, 5815; (*b*) E. Clementi and C. Roetti, *At. Nucl. Data Tables*, 1974, **14**, 177.

Paper 7/04016D; *Received* 9*th June*, 1997